Ionics (2018) 24:3845–3860
https://doi.org/10.1007/s11581-018-2529-z

ORIGINAL PAPER

The role of zirconium oxide as nano-filler on the conductivity, morphology, and thermal stability of poly(methyl methacrylate) –poly(styrene-co-acrylonitrile)-based plasticized composite solid polymer electrolytes

S. V. Ganesan[1] · K. K. Mothilal[1] · T. K. Ganesan[2]

Received: 27 September 2017 / Revised: 9 February 2018 / Accepted: 11 March 2018 / Published online: 3 April 2018

Abstract

The plasticized composite solid polymer electrolytes (CSPE) involving polymer blends poly(methyl methacrylate)-poly(styrene-co-acrylonitrile) (PMMA-SAN), plasticizers ethylene carbonate (EC), and propylene carbonate (PC) with lithium triflate ($LiCF_3SO_3$) as salt and varying concentration of composite nano-filler zirconium oxide (ZrO_2) is prepared by solution casting technique using THF as solvent. The powder X-ray diffraction (XRD) studies reveal amorphous nature of the CSPE samples. Fourier transform infrared (FT-IR) spectroscopy studies reveal interaction of Li^+ ion with plasticizers, both C=O and OCH_3 group of the PMMA, while nitrile group of SAN is inert. AC impedance and dielectric studies reveal that the ionic conductivity (σ), dielectric constant (ε'), and dielectric loss (ε") of the prepared CSPE samples increase with increasing content of ZrO_2 nano-filler up to 6 wt% and decrease with further additions. The temperature dependence of ionic conductivity follows Arrhenius relation and indicates ion-hopping mechanism. The sample Z2 (6 wt% ZrO_2) with relaxation time τ of 8.13×10^{-7} s possess lowest activation energy ($E_a = 0.23$ eV) and highest conductivity (2.32×10^{-4} S cm^{-1}) at room temperature. Thermogravimetric analysis (TGA) reveals thermal stability of highest conducting sample Z2 up to 321 °C after complete removal of residual solvent, moisture, and its impurities. Differential scanning calorimetric (DSC) studies reveal absence of glass transition temperature (T_g) corresponding to atactic PMMA for the CSPE Z2, while isotactic PMMA component shows T_g around 70 °C, which is due to increased interaction of filler with PMMA leading to change in its tacticity. Scanning electron microscopy (SEM) analysis reveals blending of PMMA/SAN polymers and lithium triflate salt. The incorporation of nano-filler ZrO_2 leads to change in surface topology of polymer matrix. Rough surface of the CSPE Z2 leads to new pathway for ionic conduction leading to maximum ionic conductivity.

Keywords Composite solid polymer electrolyte · AC impedance · Dielectric relaxation · Activation energy

Introduction

Solid polymer electrolytes are promising materials for electrochemical device applications, namely, high energy density rechargeable batteries, supercapacitors, fuel cells, electrochromic displays, etc. The polymer gel electrolytes, formed by immersing polymer in lithium salt solution containing organic solvents like THF, DMF, DMSO etc., exhibit room temperature conductivity as high as $\sim 10^{-3}$ S cm^{-1}, while dry solid polymer electrolytes (SPE) still suffer from poor ionic conductivity lower than 10^{-5} S cm^{-1} [1]. Several approaches have been adopted to enhance the room temperature ionic conductivity in the vicinity of 10^{-4} S cm^{-1} as well as to improve the mechanical stability and interfacial activity of SPEs [2, 3]. Researchers have strived hard to achieve the combination of high ionic conductivity, good electrochemical and thermal stability, as well as good mechanical properties in polymer electrolytes [4]. The poor ionic conductivity of solid polymer electrolytes can be enhanced by adding plasticizer to

Electronic supplementary material The online version of this article (https://doi.org/10.1007/s11581-018-2529-z) contains supplementary material, which is available to authorized users.

✉ K. K. Mothilal
mothi63@yahoo.com

[1] P.G. & Research Department of Chemistry, Saraswathi Narayanan College, Perungudi, Madurai, Tamil Nadu 625022, India

[2] P.G. & Research Department of Chemistry, The American College, Madurai, Tamil Nadu 625002, India

form gel polymer electrolytes, where the plasticizer effect might make the lithium salt favorably dissociated and enhance the amorphous region in polymeric matrix [5, 6]. The plasticization of a polymer electrolyte is helpful in improving the ionic conductivity by increasing the concentration of free mobile ions resulting from the reduction in viscosity of the polymer complex and increasing flexibility of the polymer backbone [7]. Weston and Steele [8] have first suggested that the dispersion of composite fillers in polymer electrolytes leads to increase in their mechanical strength. The composite fillers, e.g., Al_2O_3, TiO_2, ZrO_2, MnO_2 etc., may also act as solid plasticizers capable of enhancing the composite polymer electrolyte transport properties without affecting its interfacial stability. Further enhancement in ionic conductivity can be achieved by dispersing a nano-sized filler to form a composite solid polymer electrolyte, where the ion pairs and ion aggregates can be dissociated due to the Lewis acid-base interaction to build up a new ionic pathway for ionic transportation [9–11]. Thus, the addition of nano-sized composite fillers, along with salts in the polymer matrix, increases the ionic conductivity. The increase in the conductivity has been found to depend upon the concentration and particle size of the nano filler [12–14].

Poly(methylmethacrylate) (PMMA) is one of the polyethers extensively studied due to its ability to solvate inorganic salts to form a polymer-salt complex [15, 16]. Examples of polymer-salt complexes, PMMA–LiX, were reported by Ali et al., where X is—CF_3SO_3 (triflate) or—$N(CF_3SO_2)_2$ (bis(trifluoromethylsulfonimide)) [17]. Lithium salt is chosen for their electrochemical gain in which the cations are easily coordinated and solvated to exhibit its ionic conductivity character. In literature, there are several works on polymer blend electrolytes involving combination of crystalline or semi-crystalline polymers like PEO, PVdF, etc., and amorphous polymer like PVC, PVA, and PMMA, etc. So far, there are no reports on the polymer blend electrolytes involving both amorphous polymers. Therefore, in our present study, we have chosen two amorphous polymers, namely PMMA and SAN [poly(styrene-co-acrylonitrile)] for formation of polymer blends. G.N. Kumaraswamy et al. [18] and Miao D et al. [19] have described miscibility window at 10–30 wt% of PMMA in a PMMA/SAN blend system. Beyond 30 wt%, though the blend system is miscible yet, the hydrodynamic parameters and phase separation temperatures seem to decrease suggesting immiscibility at higher temperatures (above 160 °C). Except for the miscibility studies stated above, so far, there are no reports in the literature involving the conductivity studies on polymer electrolytes involving PMMA and SAN polymer blends. K.W. Chew et al. [20] have described more effectiveness of the solid polymer electrolyte involving PMMA and $LiCF_3SO_3$ compared to PMMA and $LiBF_4$ in terms of higher room temperature conductivity values. Moreover, lithium triflate is chosen for this study as it is a nontoxic, thermally stable salt that is miscible with organic solvents particularly THF. The plasticizers, ethylene carbonate (EC) and propylene carbonate (PC) with high dielectric constant, are added to solvate lithium ion in the polymer blend electrolyte. To this plasticized polymer blend electrolyte involving lithium triflate salt, varying concentration of nano filler ZrO_2 is incorporated in order to increase the polymer-filler interaction so that the lithium salt is free enough for conduction. ZrO_2 is an inert inorganic filler that possesses high dielectric constant similar to TiO_2 and Al_2O_3. Fillers with high dielectric constant are known to react with polymer chain. The type of interaction is dipolar and is driven by dielectric constant gradient [21]. In literature, improved ionic conductivity is observed due to the large amount of vacancies created by oxygen atoms that are available on the ZrO_2 surface and by this means tend to act as active Lewis acidic sites to interact with ions. Lewis acid site on the surface of ZrO_2 nano particle interacts with base centres of PMMA that lead to complex formation [22]. The effect of concentration of nano filler ZrO_2 on the conductivity, morphology, and thermal stability of the prepared plasticized composite solid polymer electrolyte is studied using FT-IR, XRD, AC impedance, SEM, TGA, and DSC studies.

Experimental section

Sample preparation

All the samples were prepared by solution casting technique [23]. The polymers poly(methyl methacrylate) (PMMA, Avg. $M_w = 5.5 \times 10^5$) was purchased from Alfa-Aesar and poly(styrene-co-acrylonitrile) (SAN, Avg. $M_w = 1.65 \times 10^5$) was purchased from Sigma-Aldrich and dried at 100 °C in vacuum for 10 h before use. The plasticizers, ethylene carbonate (99%) and propylene carbonate (99%), were purchased from Alfa-Aesar and used as such. The lithium triflate salt with 99.995% purity was purchased from Sigma-Aldrich and dried at 100 °C for 3 h before every synthesis. The inorganic nano filler ZrO_2 99.95% (< 100 nm) was purchased from Sigma-Aldrich and dried at 100 °C before use. The solvent tetrahydrofuran (THF) with 99.9% purity was purchased from SRL and used as such. All the apparatuses and glasswares used were dried at 100 °C before every use in order to avoid water.

In a separate conical flask, the polymers PMMA (25 wt%) and SAN (25 wt%) were blended in THF solvent. The lithium triflate (20 wt%) was blend with plasticizers ethylene carbonate and propylene carbonate in THF solvent in another conical flask and transferred to the conical flask-containing polymer blends, stirred well for few hours at room temperature. Varying concentration (wt%) of nano filler ZrO_2 (< 100 nm) in the range of 0, 5, 6, 7, 8, and 9 were added to the above

system and stirred for ~ 24 h at room temperature and at 60 °C for few hours before casting the solution onto a petri dish. The solvent tetrahyrdofuran was allowed to evaporate slowly at room temperature for 24 h until the polymer electrolyte film is formed. Now, the traces of the solvent were evaporated by drying at 70 °C in a vacuum oven for ~ 10 h. The plasticized composite solid polymer electrolytes obtained were dry, opaque, and flexible thin films. The prepared samples were labeled as Z0, Z1, Z2, Z3, Z4, and Z5 corresponding to ZrO_2 nano-filler concentration of 0, 5, 6, 7, 8, and 9 in wt% (Table 1). The CSPE samples were then transferred into a dessicator and stored till analysis.

The polymer blend (PS3) involving 50 wt% of PMMA and 50 wt% of SAN were prepared by the above procedure for morphological studies involving SEM.

The polymer blend with lithium triflate salt (PSL3) containing PMMA (40 wt%), SAN (40 wt%), and lithium triflate (20 wt%) was prepared by the above procedure for morphological studies involving SEM.

Measurements

The XRD equipment X' Pert pro PANalytical X-ray diffractometer was used for powder XRD studies. The Fourier transform infrared spectra (Shimadzu FTIR8400S) of the samples were recorded in the range 3800–500 cm^{-1}. The AC impedance measurements were carried out using HIOKI 3532 -50 LCR Hi TESTER. The parameters frequency (Hz), impedance (Z), phase angle (θ in deg), and dissipation factor (D) were obtained over a frequency range of 42 Hz–1 MHz and for temperature range of 303–373 K at every 10 K increment.

The intercept on the real axis (upon extrapolation of the slanted line in low frequency range) obtained from impedance plot of Z' vs. Z'' gives the bulk electrolyte resistance (R_b). The ionic conductivity (σ) is calculated from the measured bulk resistance (R_b) for the known area of the polymer electrolyte film with known thickness using the formula [24]:

$$\sigma\left(\mathrm{S\ cm^{-1}}\right) = (\mathrm{L/A}) \times 1/\mathrm{R_b} \quad (1)$$

where L = thickness of the CSPE film, A = area of contact.

The dielectric constant is obtained from the following formula:

$$\varepsilon' = Z''/\omega\, C_o \left(Z'^2 + Z''^2\right) \quad (2)$$

The dielectric loss is obtained from the following formula.

$$\varepsilon'' = Z'/\omega\, C_o \left(Z'^2 + Z''^2\right) \quad (3)$$

were $C_o = 8.85 \times 10^{-14}$ farad cm^{-1}, $Z' = Z\cos\theta$, $Z'' = Z\sin\theta$, and ω = angular frequency.

The thermal analysis (TGA) was performed for the sample with highest conductivity (Z2) using TA instrument SDT Q600 V20.9 Build 20 at a heating rate of 10 °C per minute from room temperature to 680 °C in nitrogen atmosphere. DSC analysis was carried out using TA instrument DSC Q20 V24.10 Build 122 analyzer in the temperature range of 0 – 200 °C at a heating rate of 10 °C per minute in nitrogen atmosphere. SEM analysis is carried out using VEGA3 TESCAN instrument to study the surface morphology of the samples.

Results and discussion

X-ray diffraction analysis

The powder X-ray diffraction measurements are carried out to study the crystalline nature and complexation behavior of the CSPE sample Z2 and compare it with nano-filler ZrO_2 and individual polymer PMMA, SAN (Fig. 1). Pure PMMA and SAN exhibit amorphous nature. The presence of broad bands with no definite crystalline peaks shows amorphous behavior [25]. The lithium triflate shows no characteristic peaks corresponding to its crystalline nature in the sample. This shows that the lithium triflate is completely dissociated and involved in interaction with the plasticizers and the polymer matrix [26]. It is evident from Fig. 1 that the CSPE sample Z2 is amorphous in nature. The presence of the peaks characteristic of nano-filler ZrO_2 in sample Z2 shows retention of crystalline nature of ZrO_2 in the amphorous polymer blend matrix. There occurs a slight shift in the 2θ values of the peak when

Table 1 Weight in (g) and its % composition for the prepared CSPE samples (Z1-Z5)

#	PMMA		SAN		EC		PC		$LiCF_3SO_3$		ZrO_2	
	g	wt%	g	wt%	g	wt%	g	wt%	g	wt%	g	wt%
Z1	0.98	25	0.98	25	0.49	13	0.45	12	0.75	20	0.19	5
Z2	0.98	25	0.98	25	0.45	12	0.45	12	0.75	20	0.23	6
Z3	0.97	25	0.98	25	0.45	12	0.42	11	0.75	20	0.27	7
Z4	0.98	25	0.98	25	0.42	11	0.42	11	0.75	20	0.30	8
Z5	0.98	25	0.97	25	0.42	11	0.39	10	0.75	20	0.34	9

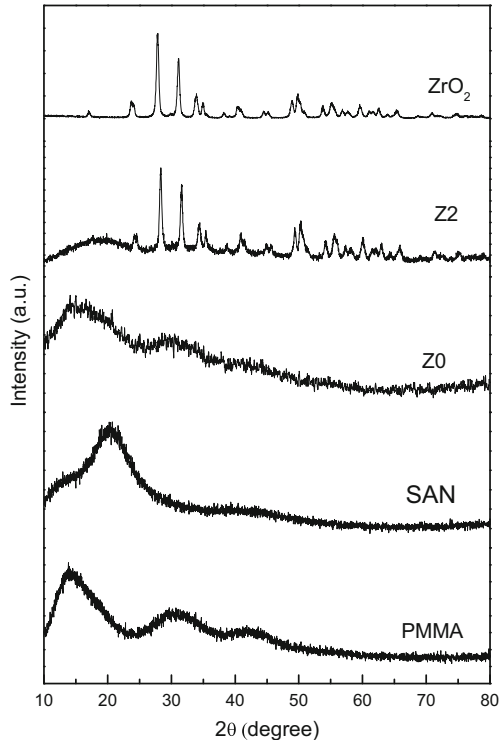

Fig. 1 XRD pattern of **a** pure PMMA, **b** pure SAN, **c** CSPE (Z2), and **d** ZrO_2

compared with X-ray diffraction pattern of nano-filler ZrO_2 (Table S1) [27, 28]. This infers that the nano-filler ZrO_2 shows strong dipolar interaction with the PMMA of the polymeric host and plasticizers [29] and retaining its crystalline nature without undergoing any structural modification or degradation.

FT-IR analysis

The FT-IR studies are carried out on the samples with maximum conductivity (Z2), minimum conductivity (Z5) and compared with pure PMMA and pure SAN (Table 2 and Fig. 2). The symmetric and asymmetric bending vibrations of SO_3 group in both samples Z2 (508 and 647 cm^{-1}) and Z5 (518 and 644 cm^{-1}) shows presence of triflate (CF_3SO_3) anion [30]. The increase in frequency of stretching and bending vibrations of C-O-C in the samples Z2 (1175 and 846 cm^{-1}) and Z5 (1171 and 846 cm^{-1}) when compared with PMMA (1117 and 842 cm^{-1}) is due to the interaction of plasticizers EC and PC with lithium ion and also due to presence of CH_2 twisting and rocking vibrations [31]. There occurs decrease in vibrational stretching frequency of C-O and C-C-O bonds in samples Z2 (1034 and 1258 cm^{-1}) and Z5 (1035 and 1259 cm^{-1}) when compared to PMMA (1061 and 1279 cm^{-1}). This indicates that the carbonyl group of PMMA and the plasticizers EC and PC containing C-O bond interacts strongly with Li^+ ion [33]. There occurs decrease in vibrational stretching frequency of $–OCH_3$ in sample Z2 and Z5 (1492 cm^{-1}) compared to (1499 cm^{-1}) PMMA [32]. Similarly, the vibrational deformation frequency of OCH_3 group shows decrease in value for Z2 (1372 cm^{-1}) and slight increase for Z5 (1388 cm^{-1}) when compared to PMMA (1387 cm^{-1}) [31]. This indicates interaction of -OCH_3 group with lithium ion and nano-filler ZrO_2 is stronger for Z2 compared to Z5. The increase in carbonyl stretching frequency for samples Z2 and Z5 (~ 1730 cm^{-1}) when compared to PMMA (1711 cm^{-1}) is due to the presence and interaction of plasticizers EC and PC along with polymer blend containing PMMA with Lithium ion [31]. There is not much change in the C=C ring stretching and C-H ring bending vibrations in samples Z2 and Z5 compared to SAN [32]. This indicates that the electron rich aromatic ring of poly(styrene-co-acrylonitrile) does not interact with either lithium ion or ZrO_2 nano-filler. The presence of C-H alkyl, alkene C-H, and aromatic group are evidenced by corresponding C-H alkyl stretching of PMMA (~ 2950 cm^{-1}), aromatic C-H stretching of SAN (3002 cm^{-1}), and alkene C-H stretching of styrene component of SAN (3027 cm^{-1}) [35]. The nitrile stretching frequency of acrylonitrile in samples Z2 and Z5 (2236 cm^{-1}) is retained when compared with (2236 cm^{-1}) (SAN) [30]. The non-polar nature of the styrene present in the SAN prevents the C≡N group of acrylonitrile from interaction with Li^+ ion as well as nano-filler ZrO_2. Weak bands with transmission intensity at 97.5%T around 3500 cm^{-1} for sample Z2 is assigned to –OH stretching that comes from ZrO_2 filler as reported for several inorganic fillers like SiO_2, TiO_2 literatures [36]. Also, weak broad bands around 3400 cm^{-1} are also characteristic of PMMA [38]. The oxygen present in ZrO_2 may interact with hydrogens of the PMMA side groups and the plasticizers EC and PC resulting in weak hydrogen bonding that leads to weak broad band at around 3500 cm^{-1} [37]. It is also observed that the intensity of this band increases with increase in ZrO_2 filler content. In the case of sample Z5 (9 wt% ZrO_2), it gives rise to band with higher intensity at around 3500 cm^{-1} compared to Z2.

AC impedance analysis

Figure 3a shows complex AC impedance spectra of the prepared composite polymer electrolytes with varying concentration of nano-filler ZrO_2 (0 wt%, 5–9 wt%) respectively. There occurs a well-defined semicircle in the high frequency region before a slanting spike in the low frequency region for sample Z0 (without nano-filler ZrO_2). The observed intercept of the plot in the high frequency semicircular region has been associated with the ionic conductivity process in the bulk of the composite polymer electrolytes. It is equivalent to the parallel combination of bulk resistance and bulk capacitance. The low frequency spike has been attributed to the blocking double-layer capacitance near the electrode/electrolyte interface due to ion migration [39]. There is either absence or very

Table 2 Assignment of FT-IR vibrational peaks (in cm^{-1}) for PMMA, SAN, CSPE Z2, and CSPE Z5

PMMA	SAN	Z2	Z5	Inference	Reference
		508	518	Symmetric bending δ_s (SO_3)	[30]
		647	644	Asymmetric bending δ_{as} (SO_3)	[30]
842		846	846	C-O-C bending, CH_2 rocking	[31]
988		911	912	CH_2 wagging	[32]
1061		1034	1035	C-O stretching	[33]
1117		1175	1171	CH_2Twisting, C-O-C stretching	[32, 34]
1279		1258	1259	C-C-O stretching	[33]
1387		1372	1387	O-CH_3 deformation	[31]
	1452	1449	1451	C=C ring breathing	[32]
1499	1494	1492	1492	C-H ring bending, O-CH_3 stretching	[32]
1711		1730	1729	C=O stretching	[31]
	2236	2237	2237	C≡N stretching	[32]
2957		2951	2952	CH_3 stretching	[35]
	3002	3003	3002	Aromatic C-H stretching	[35]
	3027	3026	3026	Alkene C-H stretching	[32]
		3532	3507	O-H stretching of surface hydroxyl groups in ZrO_2 filler	[36, 37]

negligible semicircle followed by slanting spike in the high frequency region for samples containing nano-filler ZrO_2 (Fig. 3b). The reduction or disappearance of semicircle in the high frequency region as the concentration of filler increases leads one to conclude that the majority current carriers and the conduction in electrolyte are contributed by ions and not electrons [40].

Concentration dependence conductivity

Ionic conductivity increases with increasing content of ZrO2 nano-filler up to 6 wt% and decreases further (Fig. 4). The maximum ionic conductivity of 2.32×10^{-4} S cm^{-1} at room temperature and 6.59×10^{-4} S cm^{-1} at 70 °C is obtained for sample Z2 (6 wt% ZrO_2) respectively and is comparable with similar systems in literature [20, 31, 32, 36]. The increase in ionic conductivity is due to increase in charge carriers in the polymer matrix of the electrolyte [41, 42]. The enhancement of ionic conductivity is due to interaction of the filler with lithium triflate, thereby reducing ion pairing and increasing the charge carrier density [43]. However, further addition of nano-filler ZrO_2 leads to agglomeration of the filler and reduction in the free volume leading to decreased conductivity of ions.

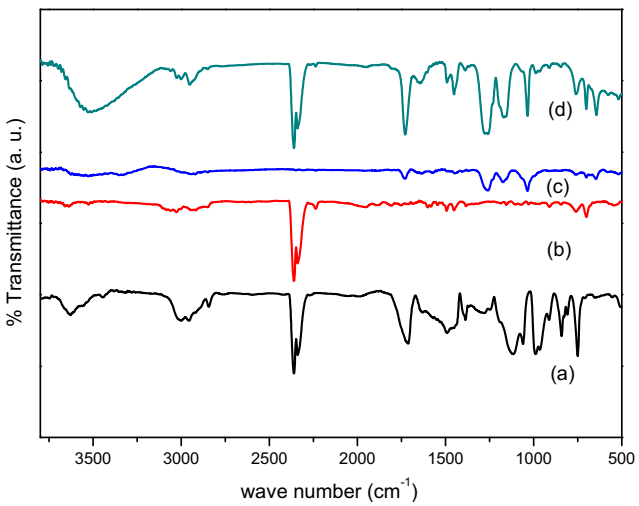

Fig. 2 FT-IR spectra of **a** PMMA, **b** SAN, **c** CSPE (Z2), **d** CSPE (Z5)

Temperature dependence conductivity

The values of ionic conductivity at different temperatures (303–343 K) as a function of nano-filler ZrO_2 concentration in the prepared CSPE samples are listed in Table 3. The logarithmic plot of variation of conductivity as function of reciprocal of temperature for different concentration of nano-filler ZrO_2 in the prepared CSPE samples is shown in Fig. 5. The linear variation of conductivity with respect to 1/T for all prepared samples shows Arrhenius behavior. Thus, variation of conductivity (σ) with temperature (T) can be considered by the relation [44]:

$$\sigma = \sigma_0 \exp\left(-E_a/\mathrm{KT}\right) \quad (4)$$

were σ_0, E_a, and K refers to the pre-exponential factor, activation energy, and Boltzmann constant respectively. This observation can be explained by ion-hopping mechanism. As the temperature increases, the conductivity also increases. Therefore, the vibrational mode of polymer segments increases and gain sufficient energy to push against the hydrostatic pressure, imposed by its surrounding atoms and turns to the formation of voids [45]. At the same time, the polymer expands to produce the free volume [46], which leads to the interaction between the electron rich carbonyl oxygen as well

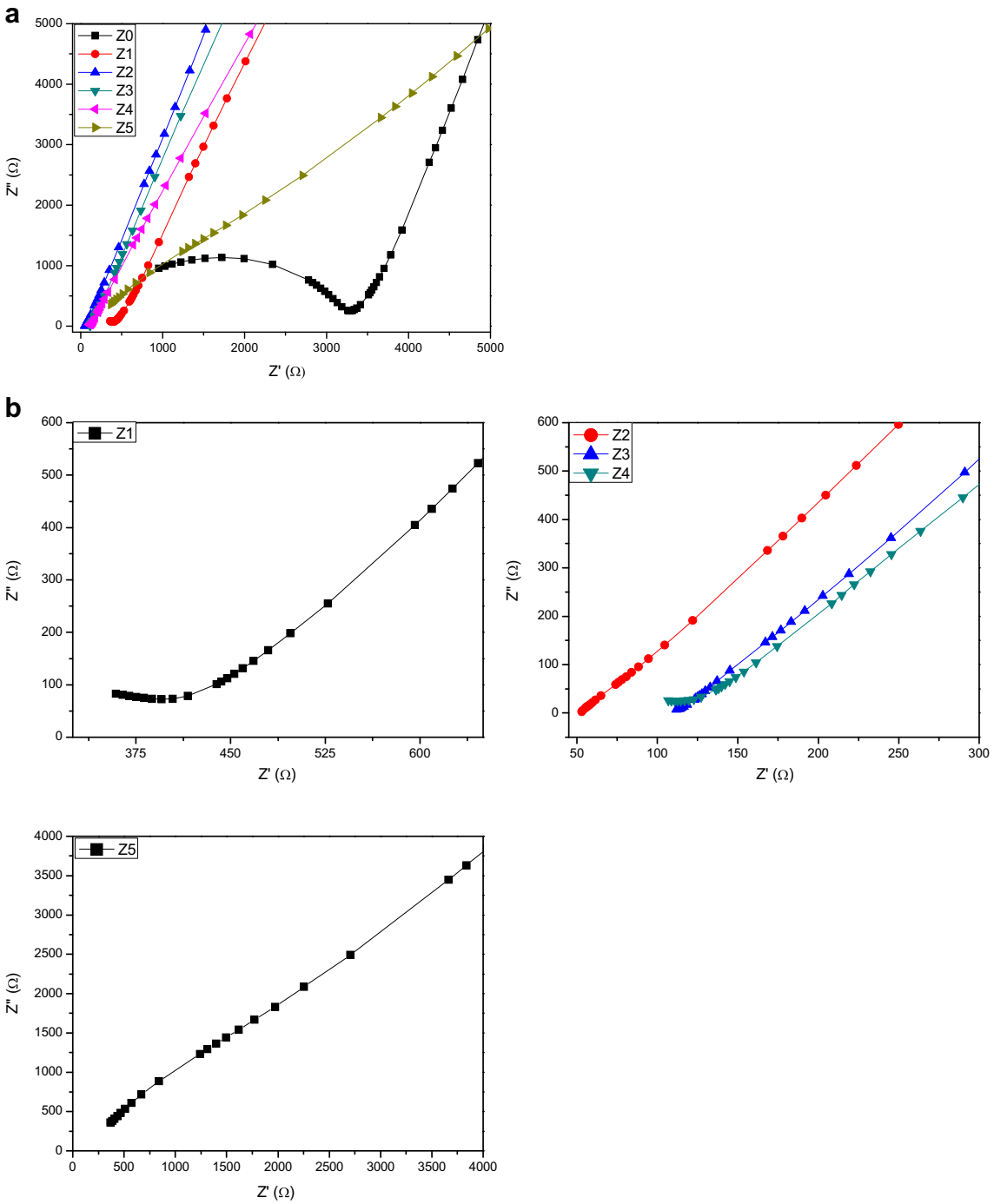

Fig. 3 **a** Impedance plot of CSPE's: PMMA-SAN-EC-PC-$LiCF_3SO_3$-xZrO_2;were $x = 0$ wt% (Z0), 5 wt% (Z1), 6 wt% (Z2), 7 wt% (Z3), 8 wt% (Z4), 9 wt% (Z5); **b** reduced coordinates of (**a**) for CSPE samples 5 wt% (Z1), 6 wt% (Z2), 7 wt% (Z3), 8 wt% (Z4), 9 wt% (Z5)

as free electrons present in the methoxy group of the polymer backbones with Li^+ ion. Thus, it promotes the charge carriers to the polymer matrix and enhances the ionic conductivity by way of segmental motion of the polymer chains [47]. The activation energy (E_a) in eV for Li^+ ion transport is calculated from the slope of the Arrhenius plot and tabulated in Table 4. The regression value is close to unity for all samples suggesting that all points lie on the straight line in Arrhenius plot.

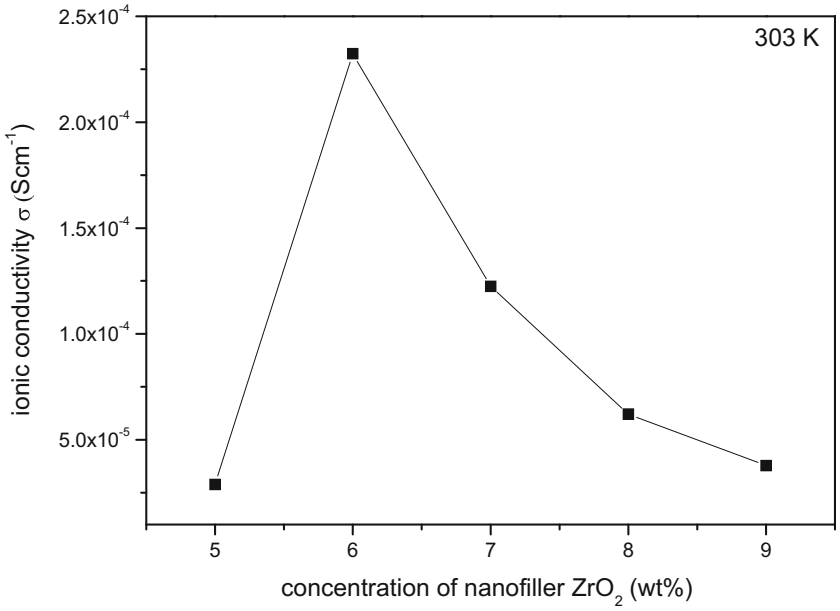

Fig. 4 Conc. of nano-filler ZrO_2 (wt%) vs. σ (S cm^{-1}) at 303 K for all CSPE samples

Figure 6 shows that when concentration of nano-filler ZrO_2 increases from 5 to 6 wt%, the activation energy (E_a) decreases. This indicates Li^+ ion has more free volume and requires less energy for migration. Hence, enhanced ionic conductivity is due to increased ionic mobility. Beyond 6 wt% of the filler, the activation energy raises as observed in samples containing 7, 8, and 9 wt% of ZrO_2 filler. This indicates more agglomeration between filler and anion of lithium salt leading to reduced free volume for lithium ion migration. Thus, sample Z2 containing 6 wt% of ZrO_2 exhibits highest conductivity of 2.32 × 10–^{4} S cm^{-1} at room temperature and possess lowest activation energy (E_a = 0.23 eV).

Dielectric studies

Dielectric study is useful in understanding the conductivity behavior of polymer electrolyte samples. This study throws light on the polarization effect at the electrode/electrolyte interface and further understanding in conductivity trend of the polymer electrolyte samples [48]. Dielectric constant (ε') is representative of stored charge in a material while dielectric loss (ε") is a measure of energy losses to move ions when the polarity of electric field reverses rapidly [49, 50]. These terms are actually real and imaginary parts of complex permittivity (ε*) and are related by the following relation.

$$\varepsilon^* = \varepsilon'(\omega) - j\,\varepsilon''(\omega) \quad (5)$$

Dielectric constant of the prepared CSPE samples increases sharply towards low frequencies with increase in the concentration of nano-filler ZrO_2 up to 6 wt% and decreases with further addition (Fig. 7). This is probably due to electrode polarization effects [51]. Higher values of dielectric constant at the low frequencies can be explained as due to the formation and accumulation of the charges (Li^+ ions) at the grain

Table 3 Variation of ionic conductivity of CSPE samples with different concentration (wt%) of nano-filler ZrO_2 at different temperatures

Sample	ZrO_2	Ionic conductivity σ (S cm^{-1})				
	(wt%)	303 K	313 K	323 K	333 K	343 K
Z0	0	1.50×10^{-6}	2.10×10^{-6}	5.00×10^{-6}	9.20×10^{-6}	1.88×10^{-5}
Z1	5	2.90×10^{-5}	4.08×10^{-5}	4.91×10^{-5}	7.72×10^{-5}	1.04×10^{-4}
Z2	6	2.32×10^{-4}	3.02×10^{-4}	3.83×10^{-4}	5.28×10^{-4}	6.59×10^{-4}
Z3	7	1.22×10^{-4}	1.76×10^{-4}	2.12×10^{-4}	3.15×10^{-4}	3.92×10^{-4}
Z4	8	6.21×10^{-5}	8.04×10^{-5}	1.12×10^{-4}	1.42×10^{-4}	1.85×10^{-4}
Z5	9	3.77×10^{-5}	5.70×10^{-5}	6.64×10^{-5}	9.13×10^{-5}	1.42×10^{-4}

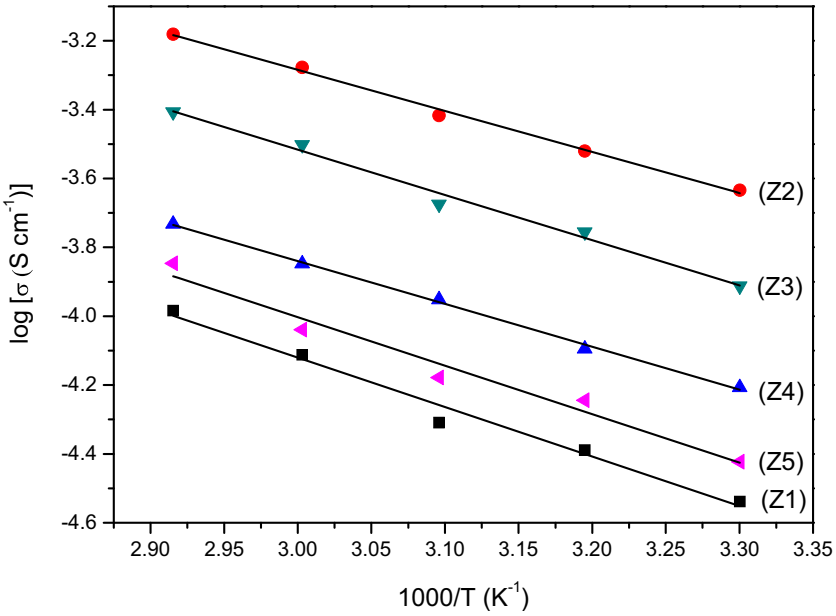

Fig. 5 Arrhenius plot for different concentration of nano-ZrO_2 filler in the prepared CSPE samples: Z1 = 5 wt%, Z2 = 6 wt%, Z3 = 7 wt%, Z4 = 8 wt%, Z5 = 9 wt%

boundaries involving polymer, nano-fillers (ZrO_2), and also at the interfaces between the electrolyte and the electrode (known as space charge polarization). At high frequencies, the periodic reversal of the electric field occurs so fast that there is no excess ion diffusion in the direction of the field. The polarization due to low charge accumulation at the electrode-electrolyte interface, leading to the observed decrease in the value of dielectric constant [52]. This is well-known as the non-Debye type of behavior, where the ion diffusion explains the space charge regions with respect to the frequency .

Figure 8 shows that the dielectric loss decreases with increase in frequency in the low frequency region followed by a peak in mid-frequency region (~4–5). At high frequency region, the dielectric loss values drop to zero. This behavior is well explained by relaxation phenomena involving polymer chain segments and the filler. The peak in the lower frequency region is known as α-relaxation [38]. The α-relaxation refers to the segmental motion of the polymer back bone chain that leads to inter-chain interactions between polymer segments [53]. Absence of peaks in the lower frequency region suggests no inter-chain interactions between polymer segments. β-relaxation refers to the appearance of peaks in the mid-frequency region due to relaxation of PMMA side-chain groups involved in interaction with filler particles [54]. The CSPE sample Z2 with 6 wt% of ZrO_2 shows β-relaxation peak at maximum height due to increased interaction between filler and the side groups of the PMMA polymer chain. This increased interaction leads to change in tacticity of PMMA from atactic to isotactic as observed in DSC analysis. Also, increased polymer-filler interaction leads to decrease in the interaction of Li^+ ion with polymer chain segments. Thus, the free solvated Li^+ ions which are known as free charge carriers show increased ionic mobility. The Li^+ ions also make use of the basic sites (oxygen atom) of the filler for its transport apart from C=O and OCH_3 groups on the PMMA. This leads to increase in the mobility of lithium ions as observed in enhanced conductivity [55].

Table 4 Activation energy (E_a) with regression coefficient for different concentration of nano-filler ZrO_2 in the prepared CSPE samples

Sample	ZrO_2 wt%	Activation energy E_a (eV)	Regression value
Z1	5	0.28	0.97
Z2	6	0.23	0.99
Z3	7	0.24	0.99
Z4	8	0.26	0.98
Z5	9	0.27	0.96

Loss tangent spectra

The dielectric relaxation parameter of the prepared CSPE samples can be obtained from study of dielectric loss tangent (tan δ) as a function of angular frequency (ω). The dielectric loss tangent (tan δ) is given by the relation:

$$\tan\delta = \varepsilon^{\wedge}/\varepsilon^{'} \quad (6)$$

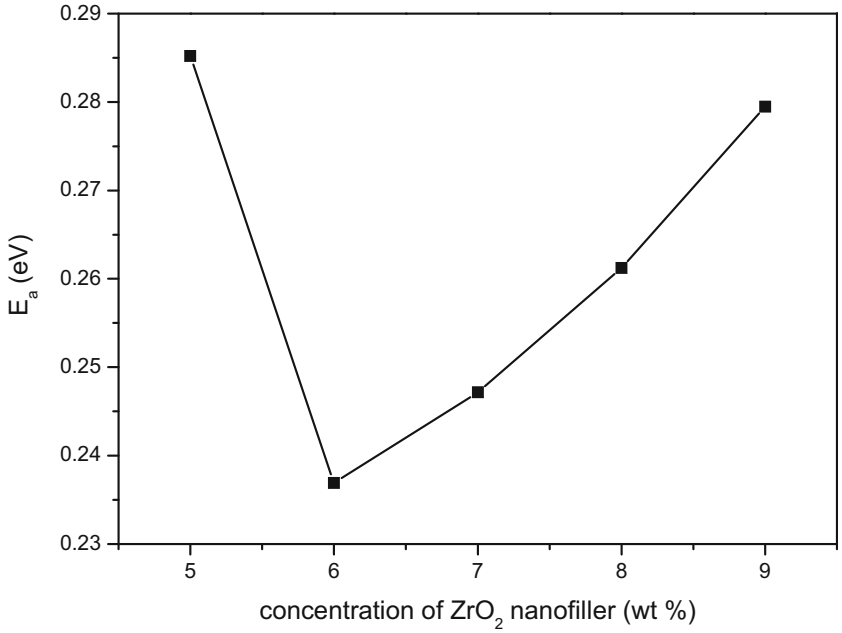

Fig. 6 Concentration of nano-filler ZrO_2 (in wt%) vs activation energy E_a for all prepared CSPE samples

It is observed that the dielectric loss tangent increases with increase in angular frequency and reaches a peak value. Further increase in angular frequency leads to decrease in the dielectric loss tangent values. The dielectric relaxation time (τ) can be obtained from the angular frequency (ω) corresponding to dielectric loss tangent (tan δ) peak as follows:

$$\omega\tau = 1 \tag{7}$$

Thus, dielectric relaxation time (τ) = $1/\omega$.

The dielectric relaxation time (τ) for different concentration of nano-filler ZrO_2 in the prepared CSPE samples are calculated from the dielectric loss tangent spectra depicted in Fig. 9. The obtained angular frequency (ω) and dielectric relaxation time (τ) are tabulated in Table 5. From the Fig. 9, it is observed that the dielectric loss tangent peak shows maximum height for the most conducting sample Z2. The loss tangent spectra show maximum angular frequency for 8 wt% of the filler.

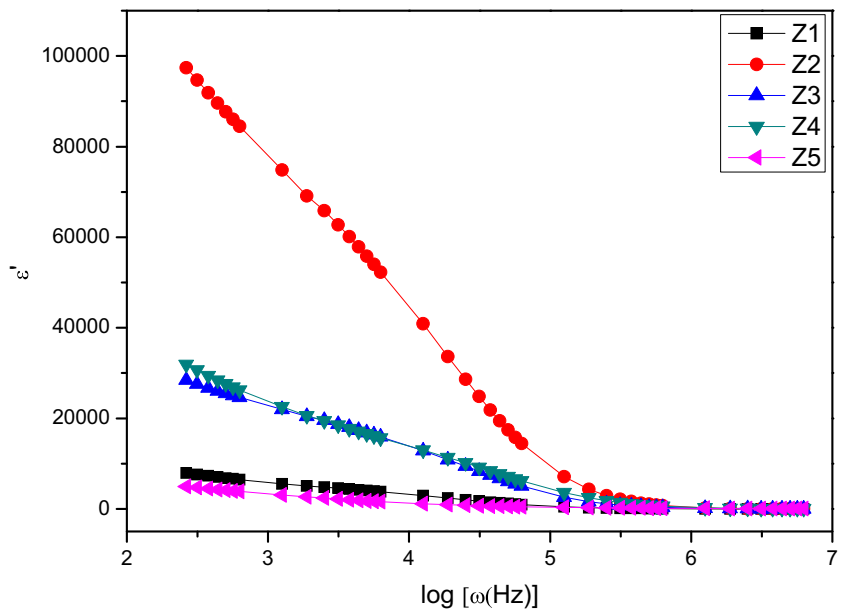

Fig. 7 Variation of real part of dielectric constant (ε') as a function of angular frequency (ω) for different concentration of ZrO2 nano-filler in the prepared CSPE samples: Z1 = 5 wt%, Z2 = 6 wt%, Z3 = 7 wt%, Z4 = 8 wt%, Z5 = 9 wt%

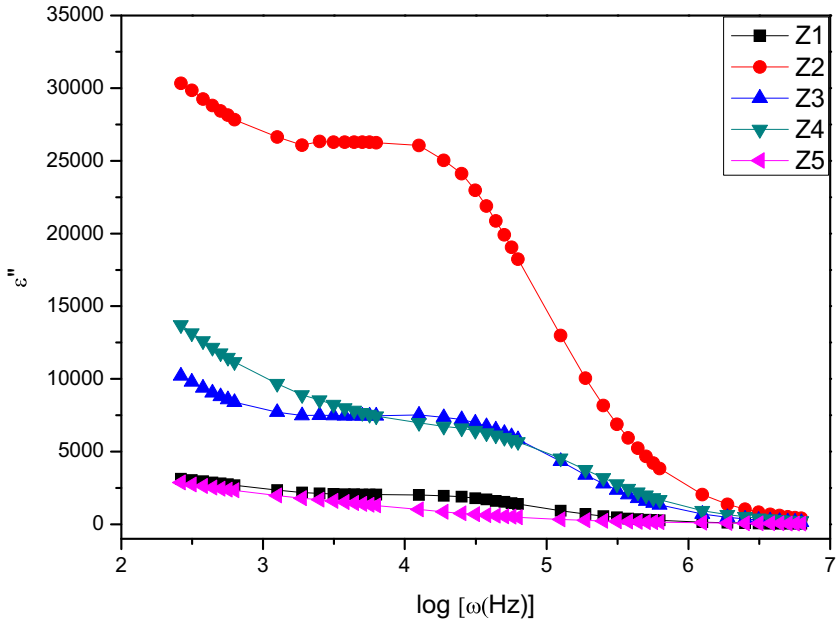

Fig. 8 Variation of imaginary part of dielectric constant (ε") as a function of angular frequency (ω) for different concentration of ZrO2 nano-filler in the prepared CSPE samples: Z1 = 5 wt%, Z2 = 6 wt%, Z3 = 7 wt%, Z4 = 8 wt %, Z5 = 9 wt%

The other peaks shift towards lower angular frequency as the filler concentration increases from 5 to 7 wt% and 9 wt% respectively (Table 5). Higher the angular frequency, shorter is the relaxation time. The sample Z4 possess shortest relaxation time (3.24×10^{-7} s). But still the sample with highest conductivity Z2 also possess relatively closer relaxation time (8.13×10^{-7} s). Thus, ionic conductivity not only depends on the number density of lithium ions but also on other factors like ionic mobility and strong correlation between the fast segmental motion of the polymer chain and mobility of both lithium ion and its counterpart, i.e., triflate anion. In the case of sample Z2, strong coordination between triflate anion and the filler leads to fast and effective

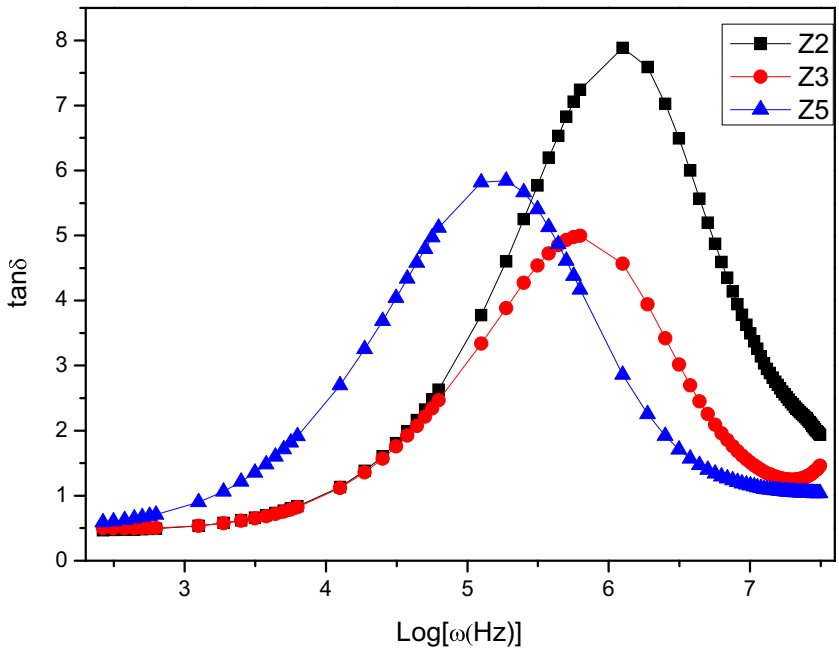

Fig. 9 Variation of tan δ as a function of angular frequency (ω) for different concentration of ZrO2 nano-filler in the prepared CSPE samples: Z2 = 6 wt%, Z3 = 7 wt%, Z5 = 9 wt%

Table 5 Relaxation time (τ) for the prepared CSPE samples at room temperature

Sample	ZrO_2 (wt%)	Angular frequency (ω_{max}) (Hz)	Relaxation time (τ) (s)
Z1	5	1.86×10^6	5.38×10^{-7}
Z2	6	1.23×10^6	8.13×10^{-7}
Z3	7	6.16×10^5	1.62×10^{-6}
Z4	8	3.09×10^6	3.24×10^{-7}
Z5	9	1.86×10^5	5.38×10^{-6}

anion transport, which is very essential for lithium ion transport and leads to enhanced transport properties of the polymer electrolyte system [56].

Thermal studies

Figure 10 represents TGA plot of highest conducting plasticized composite solid polymer electrolyte sample Z2 (6 wt% ZrO_2 filler). The TGA curve shows gradual weight loss of 4% up to 100 °C for sample Z2. The initial weight loss may be due to the presence of trace solvent and little moisture while loading the sample [32]. The further 11% weight loss takes place at 321 °C that is due to degradation of plasticizers EC and PC with boiling point around 240 °C. The drastic weight loss of 56% takes place at 435 °C with maximum degradation of polymer and plasticizer components at 389 °C [57]. Further weight loss of 14% is observed up to 491 °C with maximum degradation at 458 °C. The melting point of lithium triflate is 423 °C. Decomposition of lithium triflate takes place in this region. The final residue is around 15% that contains residue Lithium, carbon and ZrO_2 filler.

DSC analysis

From Fig. 11, DSC analysis provides the glass transition temperature (T_g) values of pure PMMA is at 62 °C for isotactic component and 120 °C for atactic component [58]. The glass transition temperature of SAN is at 100 °C respectively. The incorporation of plasticizers EC and PC into the above system involving PMMA, SAN, and lithium triflate leads to complete miscibility, and thus exhibits only one T_g value at 107 °C in sample Z0 [59]. This shows that the plasticizers help to solvate the lithium ions and make it miscible with polymer blend system by providing more amorphous rich phase [60]. In the presence of nano-filler ZrO_2 (6 wt%), the CSPE Z2 exhibits only one glass transition temperature at 70 °C. It resembles crystallization peak, suggesting the more ordered isotactic component of PMMA being formed upon interaction with the ZrO_2 nano-filler [61]. The T_g of atactic PMMA around 120 °C is not observed in Sample Z2 [58]. Surprisingly, in sample Z0, the big broad endothermic peak at 70 °C is absent which

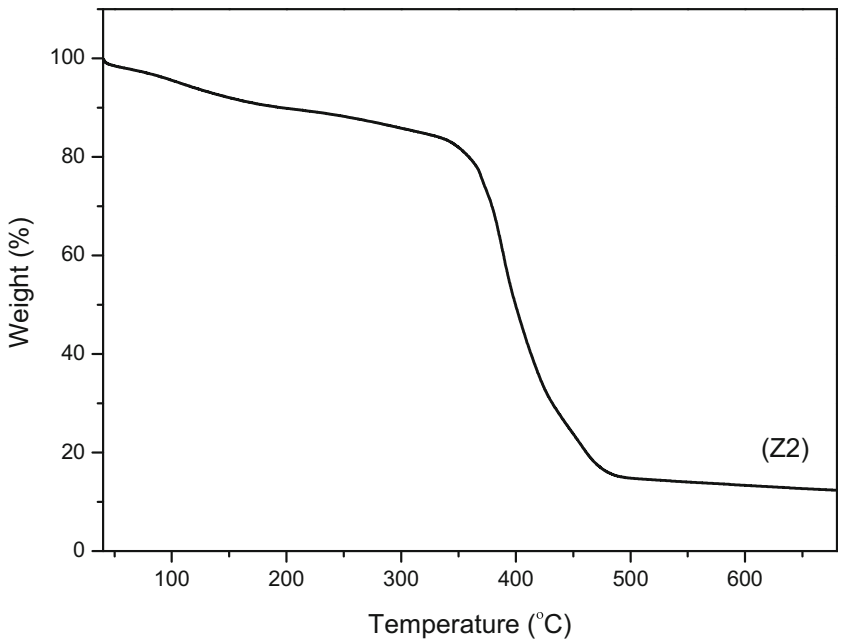

Fig. 10 Thermogravimetric analysis of maximum conducting sample CSPE (Z2)

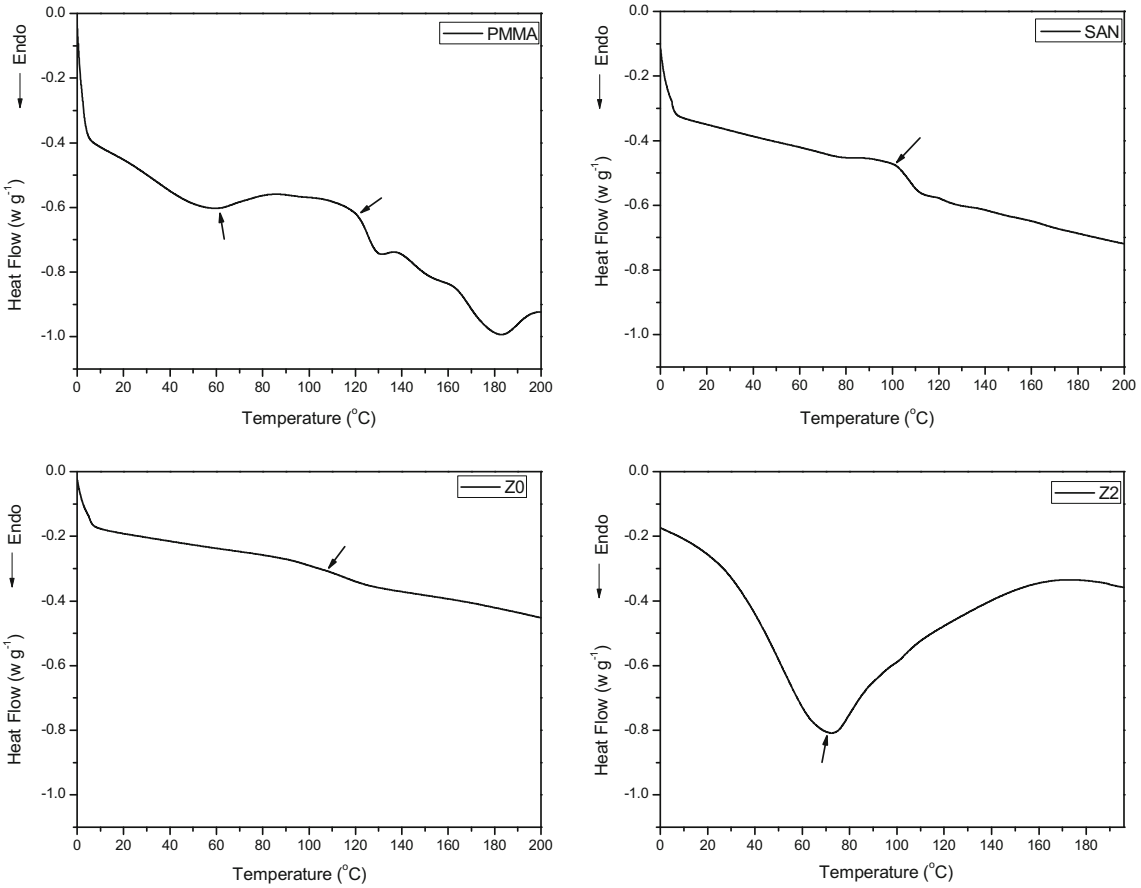

Fig. 11 DSC curves of **a** pure PMMA, **b** pure SAN, **c** CSPE (Z0), and **d** CSPE (Z2)

confirms that it is due to PMMA-filler interaction. This shows that incorporating crystalline nano-filler ZrO_2 does influence upon tacticity of the PMMA in polymer electrolyte system. Since only the syndiotactic PMMA is crystalline whose T_g is around 130 °C, and it is not formed in Z2 suggest the polymer electrolyte system is still amorphous but with improved short-range order for lithium ion transport. Therefore, lithium ion makes use of both isotactic PMMA and the basic site on the ZrO_2 for its movement. The interaction of nano-filler with the lithium and triflate ion prevents ion aggregation and enhancing further dissociation of ion aggregates leading to increased charge carrier density and ionic mobility [62].

SEM analysis

The surface morphology of the CSPE with high (Z2) and low conductivity (Z5) with maximum filler concentration (9 wt%) are compared with that of PMMA-SAN blend (PS3) and PMMA + SAN + $LiCF_3SO_3$ (PSL3) blends in the Fig. 12 through SEM micrographs. SEM analysis throws light on the surface morphology, formation of grains, and gives information on the pores and irregularities present on the polymer electrolyte surface. Thus, surface morphology influences ionic conductivity as well as stability of the polymer electrolyte films.

Figure 12a shows SEM micrograph of sample PS3 which is perfectly smooth with no pores, irregularities, and grains. This indicates perfect blend of the two polymers PMMA and SAN [63]. The addition of lithium triflate salt to the system also shows its presence at the same magnification (Fig. 12b) [32]. The morphology of the polymer surface is totally altered by the presence of filler. The CSPE sample Z2 (6 wt% ZrO_2) shows presence of lithium salt and filler on the rough polymer matrix (Fig. 12c). The rough surface of the polymer matrix provides better surface exposure for lithium ion conduction [31]. Thus, the ionic mobility is enhanced in the sample Z2. The CSPE sample Z5 (9 wt% ZrO_2) shows surface morphology in which the nano-filler ZrO_2 and lithium triflate salt are blended on to the polymer electrolyte surface. The absence of rough surface topology and the presence of smooth homogenous surface lead to decrease in ionic migration (Fig. 12d). Thus, ionic mobility is decreased and hence the ionic conductivity.

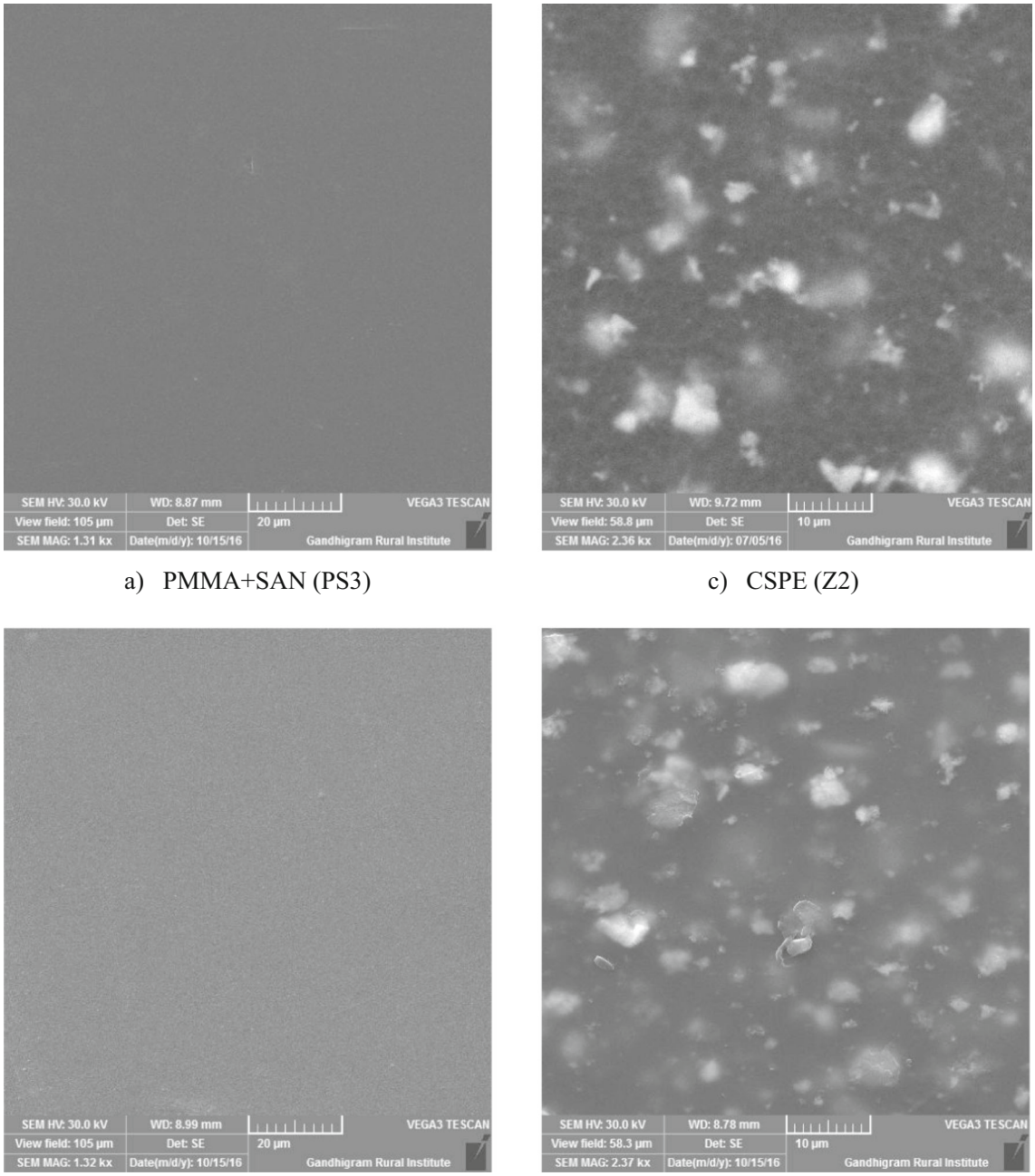

Fig. 12 Scanning electron microscope image of **a** PMMA+SAN (PS3), **b** scanning electron microscope image of PMMA + SAN + $LiCF_3SO_3$ (PSL3), **c** scanning electron microscope image of the CSPE (Z2), **d** scanning electron microscope image of the CSPE (Z5).

Conclusion

PMMA- and SAN-based composite solid polymer electrolytes involving plasticizers EC and PC with lithium triflate as salt and varying concentration of nano-filler ZrO_2 is prepared by solution casting technique using THF as solvent. The absence of XRD peaks characteristic of lithium triflate salt in the CSPE with highest conductivity (Z2) reveal that the Li^+ ion is solvated by plasticizers and involved in interactions with the polymer blend system leading to more amorphous nature of the CSPE. The retention of crystalline nature of ZrO_2 shows no degradation or transformation in the structure of the nano-filler in the composite solid polymer electrolyte system. The observed 2 Theta shift when compared with nano-filler

ZrO_2 confirms the complexation of the nano-filler with PMMA matrix. FT-IR studies reveal interaction of Li^+ ion with plasticizers as well as both C=O and OCH_3 group of the PMMA. The C≡N group of SAN does not interact with Li^+ ion as more non-polar nature of styrene prevents nitrile group of acrylonitrile from interaction with Li^+ ion. The ionic conductivity of the prepared CSPE samples increase with increasing content of ZrO_2 nano-filler up to 6 wt% and decrease with further additions. The temperature dependence of ionic conductivity follows Arrhenius relation. Arrhenius behavior of the ionic conductivity vs. 1/T for the prepared CSPE samples indicates an ion-hopping conductivity mechanism. The dielectric studies reveal that the dielectric constant (ε') and dielectric loss (ε") increase with increasing content of ZrO_2 nano-filler up to 6 wt% and decrease with further additions. The presence of relaxation peaks in the mid-frequency region of dielectric loss spectra refers to β-relaxation suggesting enhanced interaction between side-chain groups of PMMA and the ZrO_2 filler. The study of dielectric loss tangent spectra reveals shift towards lower frequency leading to longer relaxation time τ, with increase in concentration of nano-filler ZrO_2 beyond 6 wt%. The CSPE sample Z4 possess shortest relaxation time (3.24×10^{-7} s), while sample Z2 with very close relaxation time (8.13×10^{-7} s) possess lowest activation energy ($E_a = 0.23$ eV) and highest conductivity (2.32×10^{-4} S cm^{-1}) at room temperature among the prepared CSPE samples. Thus, the increase in the concentration of nano-filler ZrO_2 up to 6 wt% leads to increase in the ionic mobility and charge carrier density that combined with polymer chain segmental motion of amorphous polymer blend involving PMMA and SAN in a plasticized (EC and PC) environment leads to enhanced conductivity of the prepared CSPE samples. TGA studies reveal thermal stability of highest conducting sample Z2 up to 321 °C after complete removal of residual solvent, moisture, and its impurities. DSC studies reveal absence of glass transition temperature (T_g) corresponding to atactic component of PMMA while the T_g at 70 °C for isotactic component of PMMA is much enhanced for the CSPE Z2 when compared with individual polymers PMMA (120 °C), SAN (100 °C), and sample Z0 (107 °C). This shows that the incorporation of nano-filler ZrO_2 leads to increased interaction with PMMA of the polymer electrolyte system. The nano-filler also interacts with the lithium triflate salt preventing ion aggregation and enhancing further dissociation of ion aggregates leading to increased charge carrier density and ionic mobility. Therefore, ionic conductivity increases with increasing content of ZrO_2 nano-filler up to 6 wt% and decrease with further additions. Morphological studies using SEM analysis reveals perfect blending of PMMA and SAN polymers. The polymer blend is also miscible with lithium triflate salt. The incorporation of nano-filler ZrO_2 brings about rough surface of the polymer matrix due to enhanced interaction. The rough surface of the CSPE sample Z2 may lead to new pathway for ionic conduction; hence, enhanced conductivity is observed. Absence of rough surface in sample Z5 with much higher concentration of nano-filler ZrO_2 leads to lower conductivity.

Funding information One of the authors (S.V. Ganesan) thanks the UGC, Govt. of India, for providing him FDP Fellowship vide sanction letter FIP-TNMK 015/002(TF) under XII Plan.

References

1. Muldoon J, Bucur CB, Boaretto N, Gregory T, Noto VD (2015) Polymers: opening doors to future batteries. Polym Rev 55:208–246
2. Thiam A, Antonelli C, Iojoiu C, Alloin F, Sanchez JY (2017) Optimizing ionic conduction of poly(oxyethylene) electrolytes through controlling the cross-link density. Electrochim Acta 240: 307–315
3. Noto VD, Lavina S, Giffin GA, Negro E, Scrosati B (2011) Polymer electrolytes: Present, past and future. Electrochim Acta 57:4–13
4. Quartarone E, Mustarelli P (2011) Electrolytes for solid-state lithium rechargeable batteries: recent advances and perspectives. Chem Soc Rev 40:2525–2540
5. Sekhon SS, Krishnan P, Singh B, Yamada K, Kim CS (2006) Proton conducting membrane containing room temperature ionic liquid. Electrochim Acta 52:1639–1644
6. Singh PK, Kim KW, Rhee HW (2009) Development and characterization of ionic liquid doped solid polymer electrolyte membranes for better efficiency. Synth Met 159:1538–1541
7. Ramesh S, Shanti R, Durairaj R (2011) Effect of ethylene carbonate in poly (methyl methacrylate)-lithium tetraborate based polymer electrolytes. J Non-Cryst Solids 357:1357–1363
8. Weston JE, Steele BCH (1982) Effects of inert fillers on the mechanical and electrochemical properties of lithium salt-poly(ethylene oxide) polymer electrolytes. Solid State Ionics 7:75–79
9. Scrosati B, Croce F, Persi L (2000) Impedance spectroscopy study of PEO-based nanocomposite polymer electrolytes. Electrochem Soc 147:1718
10. Croce F, Appetecchi GB, Persi L, Scrosati B (1998) Nanocomposite polymer electrolytes for lithium batteries. Nature 394:456–458
11. Bertasi F, Vezzu K, Giffin GA, Nosach T, Sideris P, Greenbaumd S, Vittadello M, Noto VD (2014) Single-ion-conducting nanocomposite polymer electrolytes based on PEG400 and anionic nanoparticles: Part 2. Electrical characterization. Int J Hydrog Energy 39: 2884–2895
12. Shahi K, Wagner JB (1980) Fast ion transport in silver halide solid solutions and multiphase systems. Appl Phys Lett 37:757–759
13. Do NST, Schaetzl DM, Dey B, Seabaugh AC, Shirey SKF (2012) Influence of Fe_2O_3 Nanofiller Shape on the Conductivity and Thermal Properties of Solid Polymer Electrolytes: Nanorods versus Nanospheres. J Phys Chem C 116:21216–21223
14. Xiong HM, Zhao X, Chen JS (2001) New polymer−inorganic nanocomposites: PEO−ZnO and PEO−ZnO−LiClO4 Films. J Phys Chem B 105:10169–10174
15. Ali AMM, Yahya MZA, Bahron H, Subban RHY, Harun MK, Atan I (2007) Impedance studies on plasticized PMMA-LiX [X: $CF_3SO_3^-$, $N(CF_3SO_2)_2^-$] polymer electrolytes. Mater Lett 61: 2026–2029
16. Rajendran S, Shanthi Bama V, Ramesh Prabhu M (2010) Effect of lithium salt concentration in PVAc/PMMA-based gel polymer electrolytes. Ionics 16(1):27–32

17. Ali U, Karim KJ, Buang NA (2015) A review of the properties and applications of poly (methyl methacrylate) (PMMA). Polym Rev 55(4):678–705
18. Kumaraswamy GN, Ranganathaiah C, Deepa Urs MV, Ravikumar HB (2006) Miscibility and phase separation in SAN/PMMA blends investigated by positron lifetime measurements. Eur Polym J 42:2655–2666
19. Miao D, Jianhua G, Qiang Z (2004) Dynamic rheological behavior and morphology near phase-separated region for a LCST-type of binary polymer blends. Polymer 45:6725–6730
20. Othman L, Chew KW, Osman Z (2007) Impedance spectroscopy studies of poly (methyl methacrylate)-lithium salts polymer electrolyte systems. Ionics 13:337–342
21. Agrawal RC, Pandey GP (2008) Solid polymer electrolytes: materials designing and all-solid-state battery applications: an overview. J Phys D Appl Phys 41:223001(18pp
22. Austin Suthanthiraraj S, Johnsi M (2017) Nanocomposite polymer electrolytes. Ionics 23:2531–2542
23. Ramesh S, Yi LJ (2009) Structural, thermal, and conductivity studies of high molecular weight poly(vinylchloride)-lithium triflate polymer electrolyte plasticized by dibutyl phthalate. Ionics 15:725–730
24. Sharma P, Kanchan DK, Gondaliya N (2013) Effect of ethylene carbonate concentration on structural and electrical properties of PEO–PMMA polymer blends. Ionics 19:777–785
25. Rajendran S, Mahendran O, Mahalingam T (2002) Thermal and ionic conductivity studies of plasticized PMMA/PVdF blend polymer electrolytes. Eur Polym J 38:49–55
26. Su'ait MS, Ahmad A, Hamzah J, Rahman MYA (2011) Effect of lithium salt concentrations on blended 49% poly(methyl methacrylate) grafted natural rubber and poly(methyl methacrylate) based solid polymer electrolyte. Electrochim Acta 57:123–131
27. Azli AA, Manan NSA, Kadir MFZ (2015) Conductivity and dielectric studies of lithium trifluoromethanesulfonate doped polyethylene oxide-graphene oxide blend based electrolytes. Adv Mater Sci Eng:Art Id 145735:1–10
28. Mural PKS, Banerjee A, Rana MS, Shukla A, Padmanabhan B, Bhadra S, Madras G, Bose S (2014) Polyolefin based antibacterial membranes derived from PE/PEO blends compatibilized with amine terminated graphene oxide and maleated PE. J Mater Chem A 2(41):17635–17648
29. Chen HW, Lin TP, Chang FC (2002) Ionic conductivity enhancement of the plasticized PMMA/$LiClO_4$ polymer nanocomposite electrolyte containing clay. Polymer 43(19):5281–5288
30. Kumar R, Sharma JP, Sekhon SS (2005) FTIR study of ion dissociation in PMMA based gel electrolytes containing ammonium triflate: Role of dielectric constant of solvent. Eur Polym J 41:2718–2725
31. Chew KW, Tan KW (2011) The Effects of Ceramic Fillers on PMMA-Based Polymer Electrolyte Salted With Lithium Triflate, $LiCF_3SO_3$. Int J Electrochem Sci 6:5792–5801
32. Helan Flora X, Ulaganathan M, Shanker Babu R, Rajendran S (2012) Evaluation of lithium ion conduction in PAN/PMMA-based polymer blend electrolytes for Li-ion battery applications. Ionics 18:731–736
33. Ramesh S, Ang GP (2010) Impedance and FTIR studies on plasticized PMMA–$LiN(CF_3SO_2)_2$ nanocomposite polymer electrolytes. Ionics 16(5):465–473
34. Deka M, Kumar A (2010) Enhanced ionic conductivity in novel nanocomposite gel polymer electrolyte based on intercalation of PMMA into layered LiV3O8. J Solid State Electrochem 14:1649–1656
35. TianKhoon L, Ataollahi N, Hassan NH, Ahmad A (2016) Studies of porous solid polymeric electrolytes based on PVdF and PMMA grafted natural rubber for applications in electrochemical devices. J Solid State Electrochem 20:203–213
36. Ramesh S, Wen LC (2010) Investigation on the effects of addition of SiO_2 nanoparticles on ionic conductivity, FTIR, and thermal properties of nanocomposite PMMA–$LiCF_3SO_3$–SiO_2. Ionics 16(3):255–262
37. Rajendran S, Uma T (2000) Effect of ZrO2 on conductivity of PVC-PMMA-LiBF4-DBP polymer electrolytes. Bull Mater Sci 23(1):31–34
38. Gross S, Camozzo D, Noto VD, Armelao L, Tondello E (2007) PMMA: a key macromolecular component for dielectric low-κ hybrid inorganic–organic polymer films. Eur Polym J 43(3):673–696
39. Polu AR, Rhee H-W, Kim DK (2015) New solid polymer electrolytes(PEO_{20}–LiTDI–SN) for lithium batteries: structural, thermal and ionic conductivity studies. J Mater Sci Mater Electron 26(11):8548–8554
40. Jacob MME, Prabaharan SRS, Radhakrishna S (1997) Effect of PEO addition on the electrolytic and thermal properties of PVDF-$LiClO_4$ polymer electrolytes. Solid State Ionics 104(3-4):267–276.
41. Rahman MYA, Ahmad A, Lee TK, Farina Y, Dahlan HM (2012) $LiClO_4$ salt concentration effect on the properties of PVC-modified low molecular weight LENR50-based solid polymer electrolyte. J Appl Polym Sci 124(3):2227–2233
42. Lee TK, Afiqah S, Ahmad A, Dahlan HM, Rahman MYA (2012) Temperature dependence of the conductivity of plasticized poly(vinyl chloride)-low molecular weight liquid 50% epoxidized natural rubber solid polymer electrolyte. J Solid State Electrochem 16:2251–2260
43. Rajendran S, Mahendran O, Krishnaveni K (2003) Effect of CeO_2 on Conductivity of PMMA/PEO polymer blend electrolytes. J New Mater Electrochem Syst 6:25–28
44. Samsudin AS, Isa MIN (2012) Structural and ionic transport study on CMC doped NH_4Br: a new type of biopolymer electrolytes J Appl Sci 12(2):174–179
45. Rajendran S, Sivakumar M, Subadevi R (2004) Investigations on the effect of various plasticizers in PVA–PMMA solid polymer blend electrolytes. Mater Lett 58:641–649
46. Jeon JD, Kwak SY, Cho BW (2005) Solvent-free polymer electrolytes: I. preparation and characterization of polymer electrolytes having pores filled with viscous P(EO-EC)/$LiCF_3SO_3$. J Electrochem Soc 152(8):A1583–A1589
47. Aravindan V, Vickraman P (2007) A novel gel electrolyte with lithium difluoro(oxalato)borate salt and Sb2O3 nanoparticles for lithium ion batteries. Solid State Sci 9:1069–1073
48. Shastry S, Rao KJ (1991) ac conductivity and dielectric relaxation studies in AgI-based fast ion conducting glasses. Solid State Ionics 44:187–198
49. Buraidah MH, Teo LP, Majid SR, Arof AK (2009) Ionic conductivity by correlated barrier hopping in NH4I doped chitosan solid electrolyte. Phys B Condens Matter 404:1373–1379
50. Woo HJ, Majid SR, Arof AK (2012) Dielectric properties and morphology of polymer electrolyte based on poly(ε-caprolactone) and ammonium thiocyanate. Mater Chem Phys 134:755–761
51. Mishra R, Rao KJ (1998) Electrical conductivity studies of poly(ethyleneoxide)-poly(vinylalcohol) blends. Solid State Ionics 106:113–127
52. Ramesh S, Yuen TF, Shen CJ (2008) Conductivity and FTIR studies on PEO–LiX [X: $CF_3SO_3^-$, SO_4^{2-}] polymer electrolytes. Spectrochim Acta A Mol Biomol Spectrosc 69:670–675
53. Fuchs K, Chr F, Weese J (1996) Viscoelastic properties of narrow-distribution poly(methyl methacrylates). Macromolecules 29: 5893–5901
54. Rohr KS, Kulik AS, Beckham HW, Ohlemacher A, Pawelzik U, Boeffel C, Spiess HW (1994) Molecular nature of the .beta. relaxation in poly(methyl methacrylate) investigated by multidimensional NMR. Macromolecules 27:4733–4745
55. Marcinek M, Bac A, Lipka P, Zaleska A, Zukowska G, Borkowska R, Wieczorek W (2000) Effect of Filler Surface Group on Ionic Interactions in PEG−LiClO4−Al2O3Composite Polyether Electrolytes. J Phys Chem Sect B 104:11088–11093
56. Ramly K, Isa MIN, Khiar ASA (2011) Conductivity and dielectric behaviour studies of starch/PEO+*x* wt-%NH4NO3polymer electrolyte. Mater Res Innov 15:S82–S85

57. Ramesh S, Wong KC (2009) Conductivity, dielectric behaviour and thermal stability studies of lithium ion dissociation in poly(methyl methacrylate)-based gel polymer electrolytes. Ionics 15:249–254
58. Brandrup J, Immergut EH, Grulke EA, Abe A, Bloch DR (1999) Polymer handbook, 4th edn. Wiley, New York
59. Song JM, Kang HR, Kim SW, Lee WM, Kim HT (2003) Electrochemical characteristics of phase-separated polymer electrolyte based on poly(vinylidene fluoride–co-hexafluoropropane) and ethylene carbonate. Electrochim Acta 48:1339–1346
60. Prasanth R, Aravindan V, Srinivasan M (2012) Novel polymer electrolyte based on cob-web electrospun multi component polymer blend of polyacrylonitrile/poly(methyl methacrylate)/polystyrene for lithium ion batteries—preparation and electrochemical characterization. J Power Sources 202:299–307
61. Dai Pre M, Martucci A, Martin DJ, Lavina S, Noto VD (2015) Structural features, properties, and relaxations of PMMA-ZnO nanocomposite. J Mater Sci 50:2218–2228
62. Jayathilaka PARD, Dissanayake MAKL, Albbinsson I, Mellander BE (2002) Effect of nano-porous Al2O3 on thermal, dielectric and transport properties of the (PEO)9LiTFSI polymer electrolyte system. Electrochim Acta 47:3257–3268
63. Ataollahi N, Ahmad A, Hamzah H, Rahman MYA, Mohamed NS (2012) Preparation and Characterization of PVDF-HFP/MG49 Based Polymer Blend Electrolyte. Int J Electrochem Sci 7:6693–6703